



Published in final edited form as:

Stroke. 2022 September ; 53(9): 2887–2895. doi:10.1161/STROKEAHA.121.036567.

Silent infarcts, white matter integrity, and oxygen metabolic stress in young adults with and without sickle cell trait

Yan Wang, MD¹, Kristin P Guilliams, MD, MSCI², Melanie E Fields, MD, MSCI³, Slim Fellah, PhD¹, Michael M Binkley, PhD, MS¹, Martin Reis, MD⁴, Katie D. Vo, MD⁴, Yasheng Chen, DSc¹, Chunwei Ying, BS⁴, Morey Blinder, MD⁵, Allison A. King, MD, PhD, MPH⁶, Monica L. Hulbert, MD³, Hongyu An, DSc^{1,4}, Jin-Moo Lee, MD, PhD^{1,4}, Andria L. Ford, MD, MSCI^{1,4}

¹Department of Neurology, Washington University School of Medicine, St. Louis, MO

²Division of Pediatric Neurology, Washington University School of Medicine, St. Louis, MO

³Division of Pediatric Hematology/Oncology, Washington University School of Medicine, St. Louis, MO

⁴Mallinckrodt Institute of Radiology, Washington University School of Medicine, St. Louis, MO

⁵Program in Occupational Therapy and Pediatrics, Division of Hematology and Oncology, Washington University School of Medicine and St. Louis Children's Hospital, St. Louis, MO

⁶Department of Medicine, Division of hematology/oncology, Washington University School of Medicine, St. Louis, MO

Abstract

Background—Individuals with sickle cell anemia (SCA) have heightened risk of stroke and cognitive dysfunction. Given its high prevalence globally, whether sickle cell trait (SCT) is a risk factor for neurological injury has been of interest; however, data have been limited. We hypothesized that young, healthy adults with SCT would show normal cerebrovascular structure and hemodynamic function.

Methods—As a case-control study, young adults with (N=25, cases) and without SCT (N=24, controls) underwent brain MRI to quantify brain volume, microstructural integrity (fractional anisotropy, FA), silent cerebral infarcts (SCI), intracranial stenosis, and aneurysms. Pseudocontinuous arterial spin labeling and asymmetric spin echo sequences measured cerebral blood flow (CBF) and oxygen extraction fraction (OEF), respectively, from which cerebral metabolic oxygen demand (CMRO₂) was calculated. Imaging metrics were compared between SCT cases and controls. SCI volume was correlated with baseline characteristics.

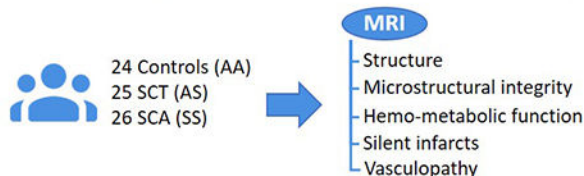
Results—Compared to controls, adults with SCT demonstrated similar normalized brain volumes (SCT 0.80 vs. control 0.81, $p=0.41$), white matter FA (SCT 0.41 vs. control 0.43, $p=0.37$), CBF (SCT 62.04 vs. control, 61.16 mL/min/100g, $p=0.67$), OEF (SCT 0.27 vs. control 0.27, $p=0.31$), and CMRO₂ (SCT 2.71 vs. control 2.70 mL/min/100g, $p=0.96$). One per cohort had an intracranial aneurysm. None had intracranial stenosis. The SCT cases and controls showed

similar prevalence and volume of SCIs; however, in the subset of participants with SCIs, the SCT cases had greater SCI volume vs controls (0.29 vs. 0.07 mL, $p=0.008$). Of baseline characteristics, creatinine was mildly elevated in the SCT cohort (0.9 vs. 0.8 mg/dL, $p=0.053$) and correlated with SCI volume ($p=0.49$, $p=0.032$). In the SCT cohort, SCI distribution was similar to that of young adults with SCA.

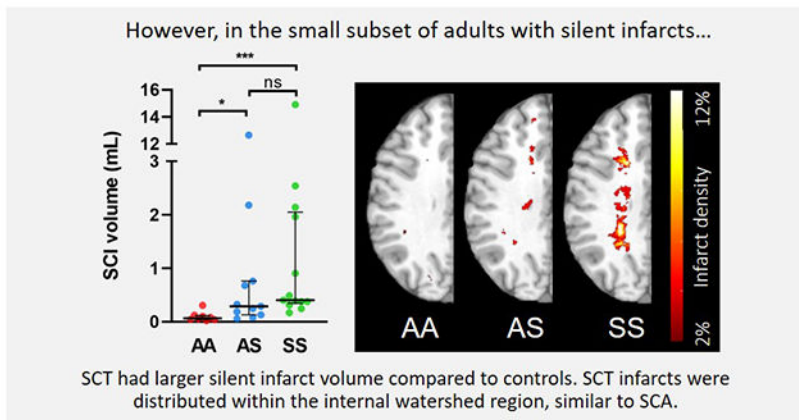
Conclusions—Adults with SCT showed normal cerebrovascular structure and hemodynamic function. These findings suggest that healthy individuals with SCT are unlikely to be at increased risk for early or accelerated ischemic brain injury.

Graphical Abstract

Is sickle cell trait (SCT) a risk factor for neurological injury?



No differences in brain volume, oxygen metabolic stress, and silent infarct burden between controls and SCT were found.



Young adults with SCT may be at low risk for early or accelerated neurological injury. Larger sample size with clinical correlation to cognitive testing is needed.

INTRODUCTION

Sickle cell anemia (SCA), caused by inheriting two copies of hemoglobin beta S (HbS) gene, affects 1 in 500 African Americans.¹ Sickle cell trait (SCT, HbAS), the heterozygous carrier state of SCA, is far more prevalent, occurring in 7 to 9% of African Americans.² In SCA, HbS polymerizes under hypoxic conditions and distorts erythrocyte shape, causing hemolysis, microvascular obstruction, and multi-organ hypoxic-ischemic injury.^{1,3} Unlike SCA, SCT is often considered a relatively benign condition; however, SCT has been linked to increased risk of chronic kidney disease,⁴ exertional rhabdomyolysis,⁵ and pulmonary embolism.⁶ While SCT carriers are relatively protected from HbS polymerization by the presence of HbA, clinically relevant sickling and ischemia may occur under extreme

conditions, such as within relatively hypoxic and acidotic environment of the renal medulla or anaerobic muscle tissue under strenuous exercise.^{7,8} In addition, SCT has been associated with a pro-thrombotic state.⁹

Despite a growing body of research investigating the neurologic ramifications of SCA, studies focusing on neurological outcomes in SCT have been limited. The association between SCT and clinically overt stroke has been debated over several decades. While case reports have described cryptogenic strokes in children with SCT,^{10,11} larger population-based cohorts of middle-aged and older adults, yielded conflicting results.¹²⁻¹⁴ A recent, large meta-analysis, which combined data from four different large cohorts, found no association between SCT and ischemic stroke;¹² however, a separate population-based cohort study found higher stroke risk in participants with SCT and concomitant chronic kidney disease.¹⁵ While metrics of cerebral atrophy, disruption in white matter microstructure, vasculopathy, cerebral blood flow, and oxygen metabolic stress have been linked to stroke and cognitive impairment in SCA, brain MRI studies in individuals with SCT have been limited.^{16,17} Due to insufficient data, historically, individuals with SCT have been excluded from control cohorts in SCA imaging studies, while their inclusion may be beneficial as a means to provide sibling controls or when matching for race and socioeconomic status.¹⁸ Furthermore, as stem cell transplant becomes increasingly utilized with siblings as ideal donors, more research is needed to study the neurological implications of effectively converting patients with SCA to SCT status.

In this study, we prospectively performed multimodal MRI to measure cerebrovascular structure, hemodynamic and metabolic function, and silent infarct burden in young adults with and without SCT. Younger participants without significant past medical history were included to mitigate the effects of age and vascular risk factors on the imaging results. Based on recent, larger epidemiologic studies showing no increase in overt stroke or dementia in older adults with SCT,^{12,17,19} we hypothesized that brain metrics of structure, microstructure, or alterations in oxygen metabolism would be similar in young, healthy adults with and without SCT. Further, we hypothesized there would be no increase in prevalence or volume of silent cerebral infarcts (SCIs) in SCT.

METHODS

Standard protocol approvals, registrations and patient consents

The studies were approved by the local institutional review board. Written informed consent was obtained from all participants. The study adhered to the STROBE statement for observational studies.²⁰ Data are available upon request from the corresponding author.

Participants

Adult, aged 18 years or older, with HbAA (controls) or HbAS (SCT cases) genotypes were enrolled as a part of a prospective, observational study. SCT status was verified through capillary gel electrophoresis. Participants were excluded for history of neurologic disease (i.e. stroke, seizures, or traumatic brain injury) or chronic medical condition (i.e. hypertension) known to increase risk of stroke. Due to difficulty with recruitment

initially, in the first half of the study, participants were allowed to be included if taking a single medication for hypertension or diabetes, however, in the second half of the study, participants were excluded if taking any medications for hypertension, diabetes and hyperlipidemia. Participants with overt strokes defined as radiographic ischemia with associated neurological deficits detectable on clinical examination were also excluded. An independent cohort of 26 young adults with SCA (HbSS genotype), enrolled concurrently with SCT participants and controls, was included for comparison of SCI volume and distribution. Participants with SCA were excluded if they had a history of stem cell transplantation, chronic transfusions, overt strokes, cerebral vasculopathy, intracerebral hemorrhage, or neurological disorder unrelated to SCA. Participants with HbAA and HbAS were siblings, partners, or friends of participants with SCA to minimize imbalance in socioeconomic status.

Labs including venous hemoglobin, capillary gel electrophoresis and venous co-oximetry, were obtained prior to each MRI. To ensure the absence of traditional vascular risk factors in this young adult population, labs including LDL, creatinine, glucose, and HbA1C were measured as well as vital signs including systolic and diastolic blood pressure and oxygen saturation (SpO₂) by pulse oximetry. CaO₂ was calculated from 1.36 x hemoglobin (g/dL) x SPO₂. Hemoglobin used in CaO₂ calculation was adjusted according to the following formula: Hb = [total measured Hb] – [total Hb x % carboxyhemoglobin] – [total Hb x % methemoglobin]. Carboxyhemoglobin and methemoglobin do not participate in oxygen exchange and were subtracted from total hemoglobin.^{21,22}

MRI protocol and image processing

MRI acquisition, segmentation, and co-registration—For the standard imaging protocol, all participants underwent brain MRI on a 3 Tesla MR system (Siemens Vision, Erlangen, Germany). Standard 3D Magnetization Prepared Rapid Gradient Echo (MPRAGE) T1-weighted (TE/TR=2.95/1800 ms, TI=1000 ms, flip angle=8°, resolution=1.0×1.0×1.0 mm), and 2D Fluid-attenuated Inversion Recovery (FLAIR) (TE/TR=93/9000 ms, TI=2500 ms, resolution=1.0×0.9×3.0 mm) were acquired. Diffusion tensor imaging (DTI) parameters were: TE/TR=89/10100 ms, resolution=2.0×2.0×2.0, 25 directions, b=0-1400 s/mm², pseudocontinuous arterial labeling (pCASL) (TE/TR=12/3780 ms, resolution=3.0×3.0×5.0 mm, labeling duration= 2000 ms, post-labeling delay=1500 ms),²³ and asymmetric spin echo (ASE), a sequence measuring tissue deoxyhemoglobin (TE/TR=64.0/4400 ms, FOV 220 mm, resolution=1.7×1.7×3.0 mm, acquisition time 7:16).²⁴

MPRAGE T1 images were skull-stripped and segmented into gray and white matter with Statistical Parametric Mapping version 12 (Wellcome Institute of Neurology, London, UK).²⁵ To limit partial volume effects, voxels with a probability less than 0.9 of being classified correctly as white or gray matter were excluded and a one-voxel morphological erosion of gray and white matter was applied to segmented images.²⁶ Co-registration aligned all images within a scan using the FMRIB Linear Image Registration Tool, with accuracy confirmed by visual inspection. White and gray matter volumes were normalized to total intracranial volume to adjust for head size. Total intracranial volume was defined as the sum of gray matter, white matter, and cerebrospinal fluid (CSF) volumes.²⁷

A board-certified neuroradiologist (M.R.), blinded to participant cohort and baseline characteristics, reviewed all MRIs and magnetic resonance angiographies (MRAs). A SCI was defined as a lesion ≥ 3 mm in diameter on fluid-attenuated inversion recovery (FLAIR) images. The neuroradiologist identified the presence or absence of cerebral aneurysms and vascular stenosis, defined as $\geq 50\%$ stenosis in any of the major intracranial vessels. For each participant with SCIs identified by the neuroradiologist, SCIs were manually delineated on the FLAIR map by a board-certified vascular neurologist (A.F.) who was also blinded to participant cohort and baseline characteristics. Voxels with SCIs were excluded from the segmented white matter mask to generate a “normal appearing white matter” (NAWM) region. This allowed for regional measurements of CBF, OEF, and DTI metrics within NAWM, unaffected by infarcts.

Diffusion tensor imaging—DTI images were processed using the FMRIB Software Library.²⁸ Briefly, for each scan, diffusion images were corrected for eddy current distortion and head motion using the $b=0$ image as a reference. A binary brain mask in DTI space was then calculated using FSL’s Brain Extraction Tool (BET) on the same $b=0$ image. Dtifit²⁹ was then applied to fit the diffusion tensor model,³⁰ generating the three principle eigenvalues at each voxel. Finally, individual mean fractional anisotropy (FA) and mean diffusivity (MD) were calculated in NAWM.

CBF and OEF image acquisition and processing—We used pCASL to measure CBF.²³ To quantify CBF, blood T1 was individually measured per participant to improve CBF reproducibility as T1 varies with age and hematocrit.³¹ Blood T1 was measured in the superior sagittal sinus and estimated using a four-parameter model as previously described.³² CBF processing did not include background suppression. The ASE sequence measuring tissue deoxyhemoglobin, was used to quantify OEF.²⁴ Quantification of voxel-wise CBF and OEF were performed as described previously.²⁴ Individual mean CBF and OEF within whole brain, gray matter, and NAWM were calculated. $CMRO_2$ within each voxel was calculated as the product of $CBF \times OEF \times CaO_2$, an equation derived from Fick’s law.³³

Silent infarct hemispheric-heatmaps—To define the location and density of infarcts for the HbAA, HbAS, and HbSS cohorts, SCI lesion masks obtained on FLAIR scans from individual cohort were aligned to the MNI-152 standard atlas space. Cohort-specific composite infarct heatmaps were created by flipping the left hemisphere onto the right hemisphere so that all infarcts were represented in a single hemisphere. Infarct density was defined as the number of hemispheres with infarcts in the voxel, divided by total number of hemispheres in the cohort, thresholded to include at least two hemispheres with infarcts in the voxel. Twenty-four control, 25 SCT, and 26 SCA participants were included in cohort-specific infarct heatmaps.

“At-risk” NAWM mask—To examine a potentially higher risk region for comparison of the imaging metrics between the HbAA controls and HbAS cases, an “at-risk” region of interest (ROI) mask surrounding SCIs was created. All SCIs from the HbAA and HbAS cohorts were combined to create an infarct mask, thresholded to two or more participants

with infarct in a voxel. The at-risk region was defined as the three-dimensional 3 mm contour surrounding the infarct mask (Figure S1). Each participant had the identical at-risk region to avoid differences due to spatial heterogeneity of given imaging metrics. The at-risk region was restricted to segmented white matter when calculating regional FA, MD, OEF and CBF.

Statistical analysis

Participant characteristics, laboratory parameters, and all continuous imaging metrics were described with median (interquartile range, IQR). Cases and controls were compared using Mann-Whitney *U* or Fisher's exact test for continuous and categorical variables, respectively. Multiple pairwise comparisons between two cohorts were calculated using Benjamini-Hochberg procedure to maintain a false discovery rate < 5%. To compare SCI volumes across the control, SCT, and SCA cohorts, Kruskal-Wallis test with Bonferroni correction was used. To examine any association between baseline participant characteristics and infarct volume, Spearman's rank correlation (ρ) was performed between SCI volume and baseline variables. Significance was determined with a value of $p < 0.05$. Multivariate linear regression analyses were used to adjust for the effects of potential confounders (age, sex, and medication usage) on continuous imaging metrics.

An *a priori* power analysis was performed based on a sample size of 25 participants per cohort. Using a non-parametric test of medians for continuous outcome variables, we had an estimated 80% power to detect an effect size of 0.83. To evaluate the likelihood of a type II error (failure to detect a true difference), we calculated minimum detectable differences (MDD) for each imaging metric to demonstrate the minimum difference between the two cohorts that we are statistically powered to detect (Table S1). Using a test based on a difference of two proportions for categorical outcome variables, we had an estimated 80% power to detect a 26% difference in event occurrence rate between the case and control groups. Statistical analyses were performed with SAS version 9.4 (SAS Institute Inc, Cary, NC).

RESULTS

Participant Characteristics

Forty-nine healthy participants with SCT (N=25) and without SCT (N=24) underwent brain MRI. Participant demographics, laboratory values, and past medical history are displayed in Table 1 and Table S2 with overall low vascular risk burden. The controls and SCT cases were well-balanced in age, sex, and race. While the two cohorts had similar hemoglobin and carboxyhemoglobin concentrations, the SCT participants had greater proportion of methemoglobin than controls (1.6 % vs 1.1%, $p = 0.039$). Systolic and diastolic blood pressure, LDL, glucose, and HbA1C, were prospectively collected, and did not differ between the two cohorts. Creatinine concentration was mildly elevated in the SCT cohort compared to controls, nearing statistical significance (0.9 mg/dL vs 0.8 mg/dL, $p = 0.053$).

Brain structure and hemodynamic function

We compared whole brain, gray matter and white matter volumes, normalized to total intracranial volume, between the two cohorts. Compared to controls, SCT cases had similar normalized whole brain, gray matter, and white matter volumes (Table 2).

To determine if white matter microstructure is disrupted in adults with SCT, we compared DTI metrics (FA, MD) between the two cohorts. Compared to controls, SCT cases had similar FA and MD (Table 2).

To examine hemodynamic and oxygen metabolic stress in children in SCT, we compared whole brain and regional CBF, OEF, and CMRO₂ in participants with and without SCT. Compared to controls, whole brain CBF, OEF, and CMRO₂ in the SCT cohort were not different (Table 2). The lack of difference between the two cohorts was consistent across gray matter and NAWM. The lack of difference between the two cohorts persisted after adjusting for age, sex, and medication usage (Table S3).

While individuals with SCA have an increased risk of developing cerebral vasculopathy, the risk in SCT is undetermined. We found similar prevalence of cerebral aneurysms between the two cohorts with one asymptomatic, intracranial aneurysm per cohort (Table 2). Cerebral arterial vasculopathy, defined as ≥ 50% intracranial stenosis, was not observed in either cohort.

Silent cerebral infarct burden and topography

We assessed SCI prevalence and volume in adults with and without SCT. The two cohorts had similar SCI prevalence (SCT, 44.0% vs control, 33%, $p = 0.56$; Table 2). SCI volume was also similar (SCT, 0.0 [0.0, 0.27] mL vs control, 0.0 [0.0, 0.05] mL, $p = 0.14$; Table 2, Figure 1A). When examining only a subset of participants who had any SCI (omitting those without SCIs), median infarct volume was greater in the SCT cases when compared to controls (SCT, 0.29 [0.13, 0.76] mL vs control, 0.07 [0.04, 0.12], $p = 0.008$; Table 2, Figure 1B). To examine whether baseline participant characteristics were associated with infarct volume, we correlated SCI volume and baseline variables within participants with SCIs. Only one baseline variable, creatinine, was significantly correlated with SCI volume ($\rho = 0.49$, $p = 0.032$). Methemoglobin, which was higher in the SCT cohort, was not associated with infarct volume ($\rho = 0.26$, $p = 0.30$). Additionally, age was not correlated with SCI volume ($\rho = 0.21$, $p = 0.39$).

To further characterize the spatial distribution of SCIs, we compared the SCT cohort to HbAA and a young adult SCA (HbSS) cohort, free of overt stroke and vasculopathy (N = 26). Clinical and radiographical characteristics of the SCA cohort, compared to HbAA and SCT cohorts, are shown in Table S3. Hemispheric infarct heatmaps for the three cohorts are represented in Figure 1. Infarcts from the SCT cohort were located in the internal borderzone and periventricular frontal white matter, with maximum infarct density of 6%. Such distribution was similar to, but less extensive than, that of the SCA cohort, which had a maximum infarct density of 12%. In contrast, infarcts in the control cohort were stochastic, located in juxtacortical white matter, with a maximum infarct density of 2%, indicating no overlap of SCIs between individuals.

Microstructural integrity and hemodynamic function in tissue “at-risk” of ischemic injury

To examine if NAWM tissue immediately surrounding SCIs was at higher risk for ischemic injury in SCT, we examined microstructural integrity, hemodynamic and oxygen metabolic stress in a 3 mm contour surrounding the SCIs (Table 2). We did not observe differences in FA and MD between SCT and controls in the at-risk region. Moreover, CBF, OEF, and CMRO₂ did not differ between the cohorts.

DISCUSSION

In this prospective MRI study, we did not detect differences in brain volume, microstructural integrity, vasculopathy, hemodynamic function, and oxygen metabolism between young adults with and without SCT. The prevalence and volume of SCIs did not differ between SCT cases and controls. Together, these findings support the hypothesis that SCT is not associated with worse neurological imaging outcomes in young adults with low burden of vascular risk factors. Logistically, our findings support the enrollment of young adults with SCT as a part of control cohorts when studying the neurological impact of SCA on brain imaging. Clinically, our study findings, if confirmed, provide reassurance to adults with SCT and their physicians that, unlike SCA, SCT is unlikely to increase the risk of neurological injury in adults who are otherwise healthy.

Our findings of normal brain volumes in SCT are supported by two recent, large population-based studies, which found no association between SCT and dementia.^{17,19} One of the studies enrolled a small subset of elderly adults into an ancillary MRI study.¹⁷ Imaging markers associated with cognitive impairment, such as gray matter volume and white matter hyperintensity volume were similar regardless of SCT carrier status.¹⁷ In contrast to our study, both population-based studies enrolled older adults with vascular risk factors. While no overall association between SCT and dementia was observed, in a secondary analysis, however, individuals with SCT and *APOE ε4* genotype, experienced greater cognitive decline than those with *APOE ε4* but without SCT.¹⁷ A similar trend was observed in individuals with SCT and diabetes compared to those with diabetes alone.¹⁷ Given the possibility of SCT acting as a genetic modifier to concomitant risk factors of cognitive decline, larger neuroimaging studies may help determine whether the presence of SCT interacts with vascular risk factors and aging to accelerate brain atrophy and microstructural impairment alongside cognitive decline.

We did not observe an overall difference in SCI prevalence or SCI volume. Similar to our findings, the MRI study ancillary to the larger community-based cohort study found no difference in white matter hyperintensity volume between aging adults with and without SCT.¹⁷ Unexpectedly, within our subset of participants with SCIs (N=19), we found greater infarct volume in the SCT cohort when compared to controls. Of baseline characteristics, serum creatinine was non-significantly elevated in the SCT cohort and significantly correlated with SCI volume. However, additional multivariable analyses aimed at interrogating potential mediators of SCI formation were limited by small sample size. The association between creatinine and SCI volume is of particular interest. SCT is not only a risk factor for chronic kidney disease,⁴ but is also a risk factor for ischemic stroke in adults with concomitant chronic kidney disease.¹⁵ Given the low sample size, our results

in this subgroup analysis should be interpreted with caution and require confirmation in a larger population. At most, these results may be hypothesis-generating, and could suggest a possible interaction between renal impairment and SCT on SCI formation. Further investigation would be required to determine if SCT act as a genetic modifier to traditional vascular risk factors.

Our results suggest no alterations to brain structure, microstructure, or oxygen metabolism in global or “at-risk” regions in the SCT cohort. In contrast, we found a discrepancy in the subset of participants with SCIs, where the SCT cohort had a larger SCI volume and its infarct pattern resembling that of the SCA cohort. To reconcile our findings, we offer the following explanations. First, SCT may have subtle alteration in oxygen metabolism from abnormalities in the oxygen dissociation curve and erythrocyte sickling,^{8,34} which may not be detected by our study, but may be detected with aging or presence of vascular risk factors. Second, as a hypercoagulable state,^{6,9} SCT may have elevated risk of cerebral micro-embolism, a mechanism of ischemia independent of oxygen metabolic stress. Embolic events would still be consistent with the watershed infarct pattern as emboli are more likely to become lodged in the low-flow watershed region and are associated with internal watershed infarcts in non-SCA patients with carotid stenosis.³⁵ Alternatively, with continued enrollment, the SCIs in the non-trait controls may eventually develop a pattern similar to SCT, involving the internal borderzone. It is likely that due to limited collateral circulation, the watershed territory is naturally prone to ischemic injury, irrespective of stroke etiology. Larger imaging studies are needed to reconcile the discrepancy between oxygen metabolic stress, microstructural integrity and SCI burden in participants with SCT.

Our study has several strengths. We applied advanced MRI methods to evaluate for any abnormalities in cerebrovascular structure and oxygen metabolic function in participants with SCT. We confirmed SCT status through direct hemoglobin electrophoresis. Our study has several limitations. While we did not detect significant differences between the HbAA and HbAS cohorts, this does not prove the absence of a difference. Based on our sample size, we were only powered to detect a difference of 26% or more for the categorical variables. We were adequately powered, however, to detect relatively small differences for the majority of our continuous imaging variables. Our results have a relatively large number of cohort comparisons and associated p-values despite the relatively low sample size. To partially address this, the Benjamini-Hochberg procedure was utilized to adjust for multiple comparisons and to minimize a false discovery rate > 5%. In addition, we did not measure serum markers of coagulation and inflammation, which may be elevated in SCT and may play a role in SCI formation.⁹ We did not collect family medical history and the enrollment of relatives may amplify genetic influences on white matter lesions, although enrolled family members were balanced across the HbAS cases and controls. Finally, in this study, we did not examine the cognitive consequences of SCIs in young, healthy adults. Prior studies on SCA suggest that even if the volume of SCI is small, its presence indicates a risk factor for ischemic injury progression and cognitive impairment^{36,37} A larger imaging study with formal cognitive testing is needed to adequately assess the clinical implications.

In conclusion, we found no differences in brain volumes, white matter microstructure, vasculopathy, cerebral oxygen metabolism, or SCI prevalence in adults with and without

SCT. Overall, young, healthy adults with SCT appear to be at low risk for early or accelerated neurological injury. Larger studies may be helpful, however, in adults with both SCT and traditional cerebrovascular risk factors to determine if their combination may interact to modify stroke risk. Logistically, the inclusion of young, healthy adults with SCT as a part of the control cohort may be permissible when studying neurological outcomes in SCA. Clinically, adults with SCT and their physicians should carefully monitor for and optimize traditional vascular risks.

Supplementary Material

Refer to Web version on PubMed Central for supplementary material.

SOURCES OF FUNDING

NIH, National Heart, Lung, and Blood Institute (R01 HL129241 [A.L.F., M.L.H.] and (K23HL136904 [M.E.F.]), and the NIH, National Institute of Neurological Disorders and Stroke (1K23NS099472-01 [K.P.G.]).

DISCLOSURES

Dr. Fields reports stock holdings in Proclara Biosciences; compensation from Montefiore Medical Center for other services; compensation from Other for other services; and employment by Washington University in St. Louis. Dr. King reports grants from National Heart, Lung, and Blood Institute and grants from Global Blood Therapeutics, Inc. Dr. An reports compensation from Pfizer Inc. for consultant services and grants from National Institute of Health. A.L. Ford, Y. Wang, K.P. Williams, S. Fellah, M.M. Binkley, M. Reis, K.D. Vo, Y. Chen, C. Ying, M.A. Blinder, A.A. King, H. An, and J-M. Lee report no disclosures relevant to the manuscript.

Non-standard Abbreviations and Acronyms

CBF	cerebral blood flow
CMRO₂	cerebral metabolic oxygen demand
DTI	Diffusion tensor imaging
HbAA	hemoglobin AA
HbAS	hemoglobin AS
HbSS	hemoglobin SS
FA	fractional anisotropy
MD	mean diffusivity
NAWM	normal appearing white matter
OEF	oxygen extraction fraction
SCA	sickle cell anemia
SCI	silent cerebral infarct
SCT	sickle cell trait

REFERENCES

1. Piel FB, Hay SI, Gupta S, Weatherall DJ, Williams TN. Global Burden of Sickle Cell Anaemia in Children under Five, 2010–2050: Modelling Based on Demographics, Excess Mortality, and Interventions. *PLoS Med.* 2013;10:e1001484. [PubMed: 23874164]
2. Ojodu J, Hulihan MM, Pope SN, Grant AM, Centers for Disease Control and Prevention (CDC). Incidence of sickle cell trait--United States, 2010. *MMWR. Morb. Mortal. Wkly. Rep* 2014;63:1155–8. [PubMed: 25503918]
3. Barabino GA, Platt MO, Kaul DK. Sickle Cell Biomechanics. *Annu. Rev. Biomed. Eng* 2010;12:345–367. [PubMed: 20455701]
4. Naik RP, Derebail VK, Grams ME, Franceschini N, Auer PL, Peloso GM, Young BA, Lettre G, Peralta CA, Katz R, et al. Association of sickle cell trait with chronic kidney disease and Albuminuria in African Americans. *JAMA.* 2014;312:2115–2125. [PubMed: 25393378]
5. Nelson DA, Deuster PA, Carter R, Hill OT, Wolcott VL, Kurina LM. Sickle Cell Trait, Rhabdomyolysis, and Mortality among U.S. Army Soldiers. *N. Engl. J. Med* 2016;375:435–442. [PubMed: 27518662]
6. Austin H, Key NS, Benson JM, Lally C, Dowling NF, Whitsett C, Hooper WC. Sickle cell trait and the risk of venous thromboembolism among blacks. *Blood.* 2007;110:908–912. [PubMed: 17409269]
7. Nath KA, Heibel RP. Sickle cell disease: Renal manifestations and mechanisms. *Nat. Rev. Nephrol* 2015;11:161–171. [PubMed: 25668001]
8. Martin TW, Weisman IM, Zeballos RJ, Stephenson SR. Exercise and hypoxia increase sickling in venous blood from an exercising limb in individuals with Sickle cell trait. *Am. J. Med* 1989;87:48–56. [PubMed: 2741981]
9. Amin C, Adam S, Mooberry MJ, Kutlar A, Kutlar F, Esserman D, Brittain JE, Ataga KI, Chang JY, Wolberg AS, et al. Coagulation activation in sickle cell trait: An exploratory study. *Br. J. Haematol* 2015;171:638–646. [PubMed: 26511074]
10. Reyes MG. Subcortical cerebral infarctions in sickle cell trait. *J Neurol Neurosurg Psychiatry.* 1989;52:516–518. [PubMed: 2738595]
11. Greenberg J, Massey EW. Cerebral infarction in sickle cell trait. *Ann. Neurol* 1985;18:354–355. [PubMed: 4051462]
12. Hyacinth HI, Carty CL, Seals SR, Irvin MR, Naik RP, Burke GL, Zakai NA, Wilson JG, Franceschini N, Winkler CA, et al. Association of sickle cell trait with ischemic stroke among African americans a meta-analysis. *JAMA Neurol.* 2018;75:802–807. [PubMed: 29710269]
13. Caughey MC, Loehr LR, Key NS, Derebail VK, Gottesman RF, Kshirsagar AV, Grove ML, Heiss G. Sickle cell trait and incident ischemic stroke in the atherosclerosis risk in communities study. *Stroke.* 2014;45:2863–2867. [PubMed: 25139879]
14. Zhang R V, Ryan KA, Lopez H, Wozniak MA, Phipps MS, Cronin CA, Cole JW, Dutta TM, Mehndiratta P, Motta M, et al. Sickle Cell Trait and Risk of Ischemic Stroke in Young Adults. *Stroke.* 2020;51:238–241.
15. Caughey MC, Derebail VK, Key NS, Reiner AP, Gottesman RF, Kshirsagar AV, Heiss G. Thirty-year risk of ischemic stroke in individuals with sickle cell trait and modification by chronic kidney disease: The atherosclerosis risk in communities (ARIC) study. *Am. J. Hematol* 2019;94:1306–1313. [PubMed: 31429114]
16. Steen RG, Hankins GM, Xiong X, Wang WC, Beil K, Langston JW, Helton KJ. Prospective brain imaging evaluation of children with sickle cell trait: Initial observations. *Radiology.* 2003;228:208–215. [PubMed: 12759471]
17. Chen N, Caruso C, Alonso A, Derebail VK, Kshirsagar AV, Sharrett AR, Key NS, Gottesman RF, Grove ML, Bressler J, et al. Association of sickle cell trait with measures of cognitive function and dementia in African Americans. *eNeurologicalSci.* 2019;16:100201. [PubMed: 31384675]
18. King AA, Rodeghier MJ, Panepinto JA, Strouse JJ, Casella JF, Quinn CT, Dowling MM, Sarnaik SA, Thompson AA, Woods GM, et al. Silent cerebral infarction, income, and grade retention among students with sickle cell anemia. *Am. J. Hematol* 2014;89:E188–E192. [PubMed: 25042018]

19. Cahill CR, Leach JM, McClure LA, Irvin MR, Zakai NA, Naik R, Unverzagt F, Wadley VG, Hyacinth HI, Manly J, et al. Sick cell trait and risk of cognitive impairment in African-Americans: The REGARDS cohort. *EClinicalMedicine*. 2019;11:27–33. [PubMed: 31312804]
20. von Elm E, Altman DG, Egger M, Pocock SJ, Gøtzsche PC, Vandenbroucke JP. The Strengthening the Reporting of Observational Studies in Epidemiology (STROBE) statement: guidelines for reporting observational studies. *J. Clin. Epidemiol* 2008;61:344–349. [PubMed: 18313558]
21. Needlemari JP, Setty BN, Varlotta L, Dampier C, Allen JL. Measurement of hemoglobin saturation by oxygen in children and adolescents with sickle cell disease. *Pediatr. Pulmonol* 1999;28:423–428. [PubMed: 10587417]
22. Caboot JB, Jawad AF, McDonough JM, Bowdre CY, Arens R, Marcus CL, Mason TBA, Smith-Whitley K, Ohene-Frempong K, Allen JL. Non-invasive measurements of carboxyhemoglobin and methemoglobin in children with sickle cell disease. *Pediatr. Pulmonol* 2012;47:808–815. [PubMed: 22328189]
23. Wu WC, Fernández-Seara M, Detre JA, Wehrli FW, Wang J. A theoretical and experimental investigation of the tagging efficiency of pseudocontinuous arterial spin labeling. *Magn. Reson. Med* 2007;58:1020–1027. [PubMed: 17969096]
24. An H, Lin W. Impact of intravascular signal on quantitative measures of cerebral oxygen extraction and blood volume under normo- and hypercapnic conditions using an asymmetric spin echo approach. *Magn. Reson. Med* 2003;50:708–716. [PubMed: 14523956]
25. Frackowiak RSJ, Frith CD, Price CJ, Ashburner JT, Friston KJ, Dolan RJ, Zeki S, Penny WD. *Human brain function*: Second edition. Elsevier Inc.; 2003.
26. Asllani I, Borogovac A, Brown TR. Regression algorithm correcting for partial volume effects in arterial spin labeling MRI. *Magn. Reson. Med* 2008;60:1362–1371. [PubMed: 18828149]
27. Wardlaw JM, Smith EE, Biessels GJ, Cordonnier C, Fazekas F, Frayne R, Lindley RI, O'Brien JT, Barkhof F, Benavente OR, et al. Neuroimaging standards for research into small vessel disease and its contribution to ageing and neurodegeneration. *Lancet Neurol*. 2013;12:822–838. [PubMed: 23867200]
28. Jenkinson M, Beckmann CF, Behrens TEJ, Woolrich MW, Smith SM. FSL. *Neuroimage*. 2012;62:782–90. [PubMed: 21979382]
29. Smith SM, Jenkinson M, Johansen-Berg H, Rueckert D, Nichols TE, Mackay CE, Watkins KE, Ciccarelli O, Cader MZ, Matthews PM, et al. Tract-based spatial statistics: Voxelwise analysis of multi-subject diffusion data. *Neuroimage*. 2006;31:1487–1505. [PubMed: 16624579]
30. Basser PJ, Mattiello J, Lebihan D. Estimation of the Effective Self-Diffusion Tensor from the NMR Spin Echo. *J. Magn. Reson. Ser. B* 1994;103:247–254. [PubMed: 8019776]
31. Jain V, Duda J, Avants B, Giannetta M, Xie SX, Roberts T, Detre JA, Hurt H, Wehrli FW, Wang DJJ. Longitudinal reproducibility and accuracy of pseudo-continuous arterial spin-labeled perfusion MR imaging in typically developing children. *Radiology*. 2012;263:527–536. [PubMed: 22517961]
32. Eldeniz C, Finsterbusch J, Lin W, An H. TOWERS: T-One with Enhanced Robustness and Speed. *Magn. Reson. Med* 2016;76:118–126. [PubMed: 26228530]
33. Valabregue R, Aubert A, Burger J, Bittoun J, Costalat R. Relation between cerebral blood flow and metabolism explained by a model of oxygen exchange. *J. Cereb. Blood Flow Metab* 2003;23:536–545. [PubMed: 12771568]
34. Becklake M, Griffiths S, McGregor M, Goldman H, Schreve J. Oxygen dissociation curves in sickle cell anemia and in subjects with the sickle cell trait. *J. Clin. Invest* 1955;34:751–755. [PubMed: 14367534]
35. Moustafa RR, Momjian-Mayor I, Jones PS, Morbelli S, Day DJ, Aigbirhio FI, Fryer TD, Warburton EA, Baron J-C. Microembolism Versus Hemodynamic Impairment in Rosary-Like Deep Watershed Infarcts. *Stroke*. 2011;42:3138–3143. [PubMed: 21852602]
36. van der Land V, Hijmans CT, de Ruiter M, Mutsaerts HJMM, Cnossen MH, Engelen M, Majoie CBLM, Nederveen AJ, Grootenhuys MA, Fijnvandraat K. Volume of white matter hyperintensities is an independent predictor of intelligence quotient and processing speed in children with sickle cell disease. *Br. J. Haematol* 2015;168:553–556. [PubMed: 25303108]

37. Jordan LC, Kassim AA, Donahue MJ, Juttukonda MR, Pruthi S, Davis LT, Rodeghier M, Lee CA, Patel NJ, DeBaun MR. Silent infarct is a risk factor for infarct recurrence in adults with sickle cell anemia. *Neurology*. 2018;91:e781–e784. [PubMed: 30054441]

Author Manuscript

Author Manuscript

Author Manuscript

Author Manuscript

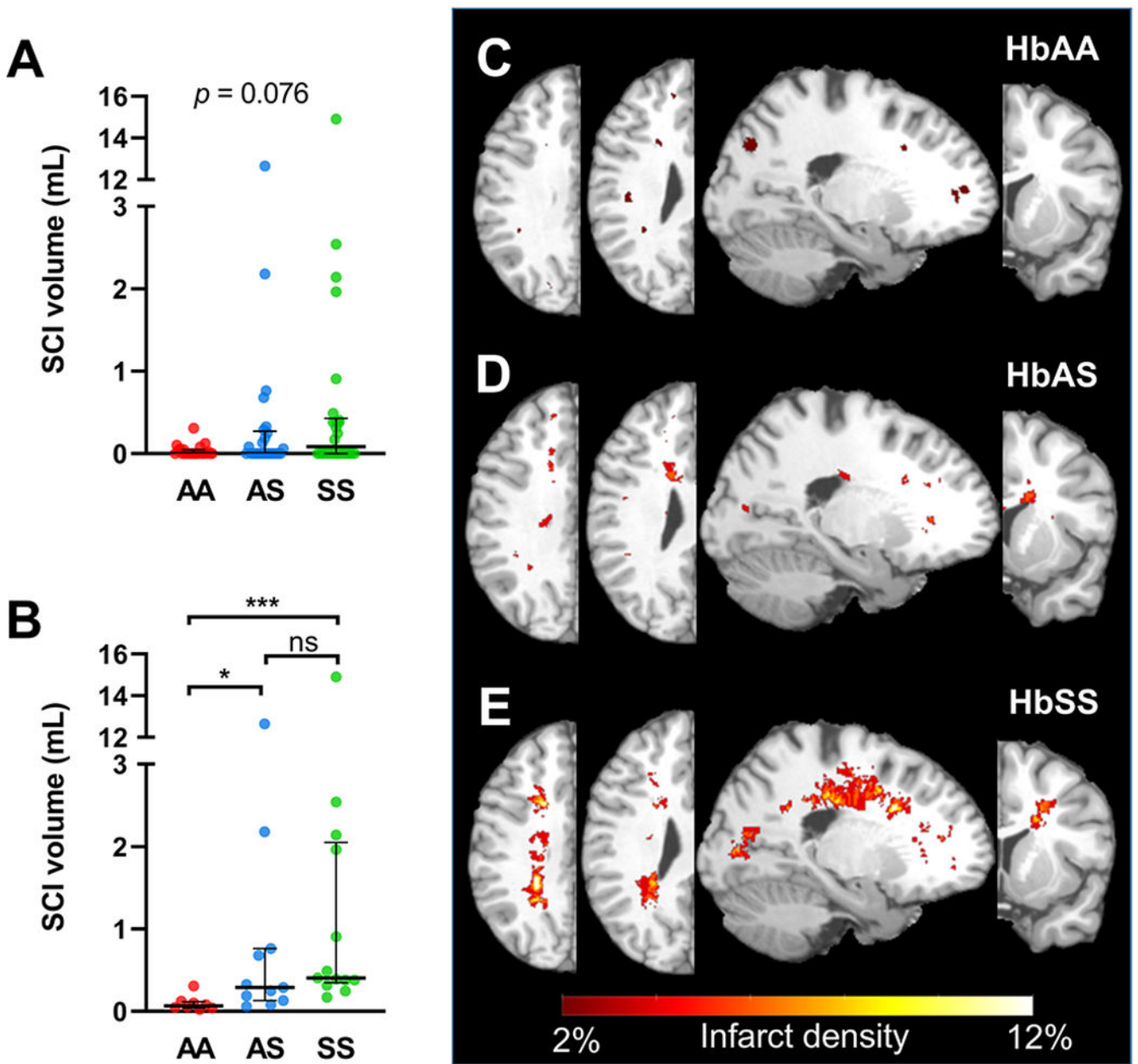


Figure 1. Silent cerebral infarct burden and pattern in young adults with and without SCT, in comparison to a SCA cohort without overt strokes.

(A) SCI volume was non-significantly different across the three cohorts ($p=0.076$). (B) Of the participants with SCIs, the SCT cohort had greater SCI volume compared to controls ($p=0.034$). Moreover, the SCA cohort had greater SCI volume compared to controls ($p=0.0004$). Hemispheric infarct density maps were calculated from FLAIR lesion maps in: (C) control, (D) SCT, and (E) SCA cohorts. Infarcts from the left hemispheres were flipped to the right hemisphere, with all infarcts represented in one hemisphere. Infarct density was defined as the number of hemispheres with infarcts in the voxel, divided by total number of hemispheres, thresholded to include two or more hemispheres with infarcts in the voxel. Infarcts from the SCT cohort were located in the internal borderzone and periventricular

frontal white matter, with maximum infarct density of 6%. Such distribution was similar, but less extensive than that of the SCA cohort, with a maximum infarct density of 12%. In contrast, infarcts in the controls were stochastic, located in juxtacortical white matter regions, with a maximum infarct density of 2% or 1 participant. Kruskal-Wallis Test was performed with significance adjusted using Bonferroni correction to maintain a family-wise error rate of 5%. ***, $p < 0.001$; *, $p < 0.05$; ns, non-significant.

Table 1:

Participant Characteristics

	HbAA (N= 24) Median (IQR)	HbAS (N = 25) Median (IQR)	p value
Age	32 (28, 36)	35 (31, 39)	0.13
Female (%)	19 (79)	18 (72)	0.74
Race, Black (%)	24 (100)	25 (100)	1
Hemoglobin, g/dl	12.35 (11.55, 13)	12.6 (12, 13.6)	0.26
COHb, %	1.0 (0.7, 2.7)	1.3 (0.8, 2.3)	0.468
MetHb, %	1.1 (0.4, 1.4)	1.6 (0.8, 1.9)	0.039
Hemoglobin A, %	97.2 (97.0, 97.4)	59.7 (57.6, 61.7)	<0.0001
Hemoglobin S, %	0 (0, 0)	37 (35.1, 39.1)	<0.0001
Hemoglobin F, %	0.4 (0, 0.4)	0.4 (0.4, 0.4)	0.007
SpO ₂ , %	100 (99, 100)	99 (98, 100)	0.19
CaO ₂ , mL/dL	16.18 (15.43, 16.96)	16.14 (15.54, 17.66)	0.72
Vascular risk factors			
SBP, mmHg	116.5 (108.5, 129)	120 (113.5, 130.5)	0.39
DBP, mmHg	73.5 (67.5, 84)	77.5 (72, 83.5)	0.45
Creatinine, mg/dL	0.8 (0.7, 0.9)	0.9 (0.8, 0.9)	0.053
Glucose, mg/dL	91 (78, 96)	94 (78, 99)	0.63
LDL, mg/dL	92.5 (77.5, 105.5)	88 (70, 111)	0.68
HbA1C, %	5.2 (5, 5.6)	5.3 (5, 5.4)	0.81
Current smokers (%) [*]	7 (32)	5 (26)	0.74

Abbreviations: COHb, carboxyhemoglobin; MetHb, methemoglobin; SpO₂, peripheral oxygen saturation; CaO₂, arterial oxygen content; SBP, systolic blood pressure; DBP, diastolic blood pressure; LDL, low-density lipoprotein; HbA1C, glycated hemoglobin.

^{*}Data available for 22 HbAA and 19 HbAS participants.

Table 2:

Brain structure, hemodynamic, and oxygen metabolic metrics in adults with and without sickle cell trait

	HbAA (N= 24) Median (IQR)	HbAS (N = 25) Median (IQR)	<i>p</i> value*
Normalized brain volume			
Whole brain	0.81 (0.77, 0.84)	0.80 (0.77, 0.82)	0.41
Gray matter	0.51 (0.47, 0.53)	0.49 (0.46, 0.52)	0.30
White matter	0.30 (0.29, 0.32)	0.30 (0.29, 0.31)	0.93
NAWM			
FA	0.43 (0.40, 0.44)	0.41 (0.40, 0.43)	0.37
MD	0.72 (0.70, 0.77)	0.72 (0.70, 0.76)	0.62
FA	0.45 (0.43, 0.46)	0.44 (0.42, 0.44)	0.10
MD	0.70 (0.67, 0.75)	0.72 (0.69, 0.74)	0.43
Hemodynamic and metabolic metrics			
Whole brain			
CBF	61.16 (54.18, 67.21)	62.04 (52.42, 64.85)	0.67
OEF	0.27 (0.26, 0.28)	0.27 (0.26, 0.28)	0.31
CMRO ₂	2.70 (2.45, 2.94)	2.71 (2.51, 2.87)	0.96
Gray matter			
CBF	68.12 (57.51, 74.86)	68.40 (55.16, 73.34)	0.72
OEF	0.29 (0.27, 0.30)	0.28 (0.26, 0.30)	0.28
CMRO ₂	2.99 (2.76, 3.49)	3.10 (2.69, 3.37)	0.96
NAWM			
CBF	37.14 (32.77, 42.17)	39.83 (33.54, 44.34)	0.39
OEF	0.25 (0.24, 0.27)	0.25 (0.24, 0.27)	0.81
CMRO ₂	1.54 (1.45, 1.71)	1.71 (1.39, 1.84)	0.27
CBF	23.63 (20.80, 27.06)	24.08 (19.42, 28.14)	0.56
OEF	0.24 (0.23, 0.25)	0.24 (0.23, 0.26)	0.87
CMRO ₂	0.94 (0.85, 1.09)	0.90 (0.75, 1.14)	0.71
Cerebral vasculopathy, N (%)	0 (0%)	0 (0%)	1
Aneurysm, N (%)	1 (4.2%)	1 (4%)	1
Silent infarct, N (%)	8 (33.3%)	11 (44.0%)	0.56
SCI volume, mL	0.0 (0.0, 0.05)	0.0 (0.0, 0.27)	0.14
SCI volume, in participants with SCI on MRI, mL	0.07 (0.04, 0.12)	0.29 (0.13, 0.76)	0.008

Abbreviations: SCI, silent cerebral infarct; NAWM, normal appearing white matter; FA, fractional anisotropy; MD, mean diffusivity, expressed in unit of $10^{-3}\text{mm}^2\text{s}^{-1}$; CBF, cerebral blood flow, expressed in unit of mL/min/100g; OEF, oxygen extraction fraction; CMRO₂, cerebral metabolic rate of oxygen, expressed in mL/min/100g.

*Raw *p* value reported with significance calculated with the Benjamini-Hochberg-adjusted *p* values to maintain a false discovery rate of 5%.